Effect of Cyclodextrin Nanocavity Confinement on the Photorelaxation of the Cardiotonic Drug Milrinone

Maged El-Kemary,[§] Juan Angel Organero, Lucia Santos, and Abderrazzak Douhal*

Departamento de Química Física, Sección de Químicas, Facultad de Ciencias del Medio Ambiente, Universidad de Castilla-La Mancha, Avda. Carlos III, S.N., 45071 Toledo, Spain

Received: March 31, 2006; In Final Form: June 5, 2006

We report on steady-state UV−visible absorption, emission, and picosecond emission studies of milrinone (MIR) drug in neutral water and complexed to cyclodextrins (α-, *β*-, *γ*-CD and dimethyl-*β*-CD (DM-*β*-CD)). The results reveal that MIR forms a 1:1 inclusion complex with CD. Upon encapsulation the emission intensity increases and the fluorescence lifetime changes from ∼65 ps to 240−350 ps, indicating a confinement effect of the nanocages on the photophysical behavior of the drug. Due to its methyl groups, the DM-*β*-CD complex shows the largest effect. The time−anisotropy experiments support the formation of 1:1 inclusion complexes and indicate motion of the drug inside the nanocavity. Furthermore, results of PM3 calculations combined with spectral and dynamical data show that the drug is not fully embedded into the cavities, and the conformation of the included complex explains the relatively short lifetimes and low emission quantum yields of these entities.

1. Introduction

Cyclodextrin (CD) nanocavities are potential candidates for drug delivery systems through the formation of inclusion complexes on the basis of noncovalent interaction.[1] The hydrophobic environment of a CD nanocavity can lead to the alteration of physical, chemical, and biological properties of guest molecules.[2−4] Understanding the dynamic aspects of caged drugs into nanocavities can be used to gain information for new formulations and a better bioavailability of the drug. The molecular mechanisms of the drug phototoxicity can be explored through the study of the fast dynamic aspects of drugs in different media, including CD cavities.[5] As already reported for a large variety of systems, a CD cavity is able to influence both the fate of the reaction intermediates and the deactivation pathways of the excited caged drugs.[5,6] This may lead to a decrease in phototoxicity.

Previously, we have reported on the fast dynamic of milrinone (MIR), 1,6-dihydro-2-methyl-6-oxo-3,4′-bipyridine-5-carbonitrile (Scheme 1), a cardiotonic drug in aqueous solution.[7] The medicine has been found to exist in different structures depending on the pH of the medium. At neutral pH, under biologically relevant conditions, the keto structure predominates.[7] The efficient nonradiative relaxation for the different structures are explained in terms of hydrogen-bonding interactions, intramolecular charge-transfer (ICT), and twisting motion.[7] Both keto and cation structures are the active forms of MIR inotropic agent.[8,9] The H-bonding, twisting motion, and ICT are perhaps key features for inotropic activity of keto and cation structures.[7] This drug used for treatment of congestive heart failure and its short response time is promising.[10−13] However, long-term investigations for oral use of the drug revealed that it is associated to adverse side effects, such as thrombocytopenia, fever, anorexia, abdominal pain, nausea, emesis, and there are some indications of increased mortality.[10−13] It is expected that the formulation of MIR within CD may show a better bioavailability, with a decrease of some of these undesirable effects.

In this contribution, we report on the effect of α-, *β*-, and *γ*-CD and DM-*β*-CD complexation on the fast photodynamics of MIR. The results show a relative increase in emission quantum yield and lifetime upon encapsulation by CD. We explain them on the basis of motion restriction and hydrophobic effect of the nanocages.

2. Experimental and Computational Details

MIR (Sigma-Aldrich), α-, *β*-, and *γ*-CD and DM-*β*-CD (Across), and spectroscopy grade tetrahydrofuran (THF, Sigma-Aldrich) were used as received. The purity of the drug was checked by thin-layer chromatography (TLC). Deionized distilled water was used for preparation of the solutions. The pH of the aqueous solutions was adjusted by adding aliquots of diluted HCl or NaOH solutions. A film of poly(methyl methacrylate) (PMMA, Sigma-Aldrich) was prepared by dissolving both MIR and PMMA in THF and evaporating the solvent under vacuum.

Steady-state absorption and emission spectra were recorded on Varian (Cary E1) and Perkin-Elmer (LS 50B) spectrophotometers, respectively. Emission decays were measured using a time-correlated single photon counting system (FluoTime 200, PicoQuant).[14] The sample was excited by a 40 ps pulsed (20 MHz) laser centered at 371 nm, and the emission signal was collected at the magic angle. The instrumental response function (IRF) of the apparatus was typically 65 ps. A multiexponential function convoluted with the IRF signal were fitted to the emission decays using the Fluofit package (Picoquant). The quality of the fits was characterized in terms of residual distribution and reduced χ^2 value. All the measurements were done at a MIR concentration of 1×10^{-5} M and at 293 ± 1 K. No degradation was observed during the measurements.

* Corresponding author. Phone: +34-925-265717. Fax: +34-925-268840. E-mail: Abderrazzak.douhal@uclm.es.

§ Permanent address: Department of Chemistry, Faculty of Science, Tanta University, 33516 Kafr ElSheikh, Egypt.

10.1021/jp062015a CCC: $33.50
Published on Web 07/06/2006

SCHEME 1: Schematic Representation of the 1:1 Inclusion Complex between 1,6-Dihydro-2-methyl-6-oxo-3,4′-bipyridine-5-carbonitrile, Milrinone (MIR), and a CD Cavity in Neutral Water

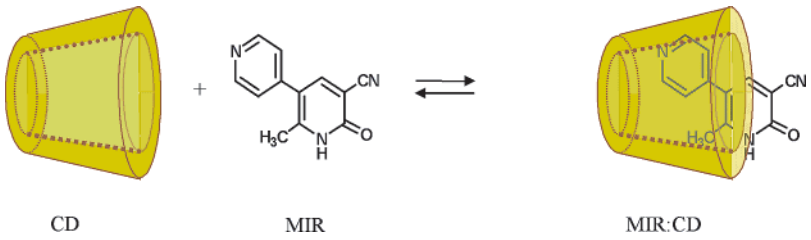

Theoretical calculations were performed with the GAUSSIAN 03 software package. The initial geometry of MIR was optimized by means of ab initio using the B3LYP/6-31+G** method.[15,16] The PM3 method is used to build and optimize the CD structure. The glycoside oxygen atoms were placed into the *XY* plane, and their center was defined as the center of the coordination system. The secondary hydroxyl groups were placed pointing toward the positive *Z* axis. The longer dimension of the guest molecule was initially placed along the *Z* axis. The position of the guest was determined by the *Z* coordinate of the carbon atom number 4 of the pyridine ring. The geometry of the host−guest complex was completely optimized by PM3 without any restriction. We have considered two kinds of inclusion mode of the formed complex. One mode in which the inclusion of MIR into CD is through the pyridyl part, and the other one is through the pyridone moiety. The inclusion angle for each complex is that between the plane of the included moiety and a perpendicular plane of the (larger) gate of CD.

3. Results and Discussion

3.1. Steady-State Absorption and Fluorescence Spectra. Figure 1A displays the UV−visible absorption spectra of MIR in neutral water and in the presence of DM-β-CD. A very small change in the spectra was detected upon addition of DM-β-CD, suggesting a weak interaction between CD and drug or a small change in the molar absorption coefficient of the drug. The most important change is around 300 nm.

Figure 1B shows the steady-state emission spectra of neutral aqueous solution of MIR and in the presence of different DM-β-CD concentrations, upon exciting at 340 nm. In water, MIR exhibits a band with a maximum at 385 nm and a fluorescence quantum yield (Φ_f) of 0.014. Upon addition of DM-β-CD, the emission intensity is enhanced with a small red shift of the band, suggesting the formation of complex between MIR and DM-β-CD (Scheme 1). For β- and γ-CD solutions, the increase in the emission intensity is weaker. Compared to water solution, MIR emission band in nonpolar and polar media (water: 385 nm, 1,4-dioxane: 397 nm and acetonitrile: 392 nm) shows a red shift. This result indicates that binding of MIR to CD changes the local solvation environment (water) in a way similar to changing the solvent from protic to aprotic medium. The polarity of medium (CD) must also play a role in its photophysics as the molecule contains polar groups. Previously, we have reported on the involvement of the ICT reaction in water solution.[7] Upon encapsulation, MIR experiences a reduced H-bonding interaction with water. For α-CD, no significant change in the fluorescence intensity was observed, suggesting no complex formation due to the small size of this cavity. In neutral water solution, MIR exists predominantly in keto (**K**) structure in agreement with theoretical calculations, which show that in a water cavity, **K** is more stable than the enol form by ∼7 kcal/mol.[7]

Analysis of the emission data (Figure 1B) assuming a 1:1 stoichiometry of the complex was performed using[17]

$$I/I_0 = (1 + KG(\Phi_c/\Phi_0)[CD])/(1 + K[CD]) \qquad (1)$$

where I and I_0 are the emission intensities with and without CD, respectively. G denotes the ratio of the molar absorption coefficients ($\epsilon_{complex}/\epsilon_{free}$) of the drug at the excitation wavelength, 340 nm. Φ_0 and Φ_c are the emission quantum yields of the free and complexed drug, respectively. Under the conditions used in this study, $[DM\text{-}\beta\text{-}CD]_0 \gg [MIR]_0$ (2−21 mM $\gg 1 \times 10^{-5}$ M), and then [CD] was replaced by $[CD]_0$ in eq 1. We also fixed $G = 1$ in the fit, as the absorption spectra suggest no change in the molar absorption coefficient at 340 nm of the drug upon complexation with DM-β-CD (Figure 1A). Fitting the data using eq 1 (Φ_c is free in the fit), we obtained $K = 30 \pm 5\ M^{-1}$, $\Phi_c = 0.076$, and $R^2 = 0.995$ for DM-β-CD solutions. The value of Φ_c/Φ_0 (5.43) deduced from the best fit is close to that of $\tau_{complex}/\tau_{free}$ (5.38), suggesting the constancy of the radiative rate constant (k_r) of the drug upon complexation. The constancy of k_r values is in agreement with the lack of change in the absorption spectra upon addition of CD. Therefore, the

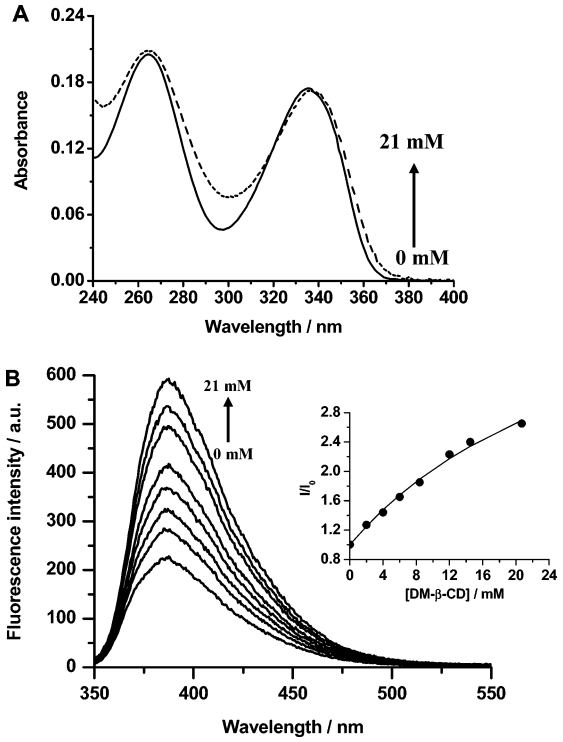

Figure 1. UV−visible absorption (A) and emission (B) spectra of MIR in water and in the presence of DM-β-CD. For the emission, the excitation wavelength was 340 nm. The inset of part B shows the variation of the relative emission intensities at 385 nm with the initial DM-β-CD concentration. The solid curve is the result of the best fitting according to eq 1.

deduced K value from the fit is reasonable. Using the same fitting procedure, we obtained $K = 22 \pm 4$ and 14 ± 3 M^{-1} for β-CD and γ-CD, respectively. The magnitude of inclusion equilibrium constant increases in the order γ-CD < β-CD < DM-β-CD. For α-CD, the binding constant is too weak to be measured. The value of Φ_c for DM-β-CD complex is almost twice that for β- and γ-CD complexes. For the former, the methyl groups act as a hydrophobic protector screen of the guest from water molecules, and restriction to possible twisting motion of both parts of the guest is more significant than in β- and γ-CD entities. The PM3 results (vide infra) support this explanation.

These results suggest that the size of CD cavity plays a role in the formation and stability of the formed complex. The molecular length of MIR is ∼9.5 Å and the width of the pyridone moiety is ∼7 Å, larger than that of α-CD diameter (∼5.7 Å). Thus, the relationship between the size of guest and the cavity of the host precludes the inclusion complex formation with α-CD. In fact, no change in the fluorescence spectra of MIR was observed after addition of α-CD. The diameter of β-CD and γ-CD are large enough (∼8 and 9.5 Å, respectively) to form a confined nanostructure. The unsubstituted CDs have similar height (∼8 Å), therefore part of the drug could still be outside the nanocage (vide infra). Due to the methyl groups, the height of DM-β-CD cavity is longer (∼11 Å).[18] The larger K value of MIR in the presence of DM-β-CD (30 M^{-1}) in comparison with β-CD (22 M^{-1}) may be due to hydrophobic part of DM-β-CD provided by the methyl groups. Similar observations have been reported for other caged molecules.[19,20] The estimated equilibrium constant values for encapsulation of MIR is not very different from those obtained for guests of similar size.[20−22] Values of 12 M^{-1} for 4-aminophthalimide:β-CD[21] and methyl-2-amino-4,5-dimethoxy benzoate:β-CD,[22] and 18.5 M^{-1} for 7-hydrxyquinoline:DM-β-CD[20] were reported. In addition to the importance of the relative size of the guest to that of the host cavity for the complex formation, the stability of the complex depends on the interplay between van der Waals and hydrophobic forces and electrostatic interactions.[23]

To get information on the conformation of the complexes, we performed PM3 calculations. The result suggests two possible inclusion modes of the guest into the cavity. One fitting mode includes the pyridyl moiety, and the other one encapsulates the pyridone part. For the first one the CN group of the nonincluded pyridone points toward the secondary hydroxyl rim of the CD cavity (largest gate), while for the second one this group points toward the primary hydroxyl rim of the cavity (smallest gate). The angle (θ) between the plane of the included moiety and that perpendicular to the gate of CD depends on the cavity size. For the first fitting mode, we found $\theta \sim 10°$ for β- and DM-β-CD, and $\theta \sim 50°$ for γ-CD. Furthermore, for β- and DM-β-CD complexes, a length of 3 and 4 Å of the pyridone part is exposed to water, respectively. For γ-CD nanostructure, the nonincluded moiety is longer: ∼5 Å. The difference in length and volume of the complexes is relevant to the rotational time of these entities in agreement with the time-resolved anisotropy data (vide infra). For the second inclusion mode, the fitting angle of the pyridone ring (almost constant) and the remaining length of pyridyl moiety are (θ, l): (5°, 2 Å), (7°, 3.2 Å), and (10°, 2.8 Å) for DM-β-, β-, and γ-CD, respectively. The fitting angle is larger for the largest cavity, and the degree of hydrophobic protection is larger for DM-β-CD, due to its methyl groups.

The first inclusion mode gives the most stable complex for β-, DM-β-, and γ-CD cavities. When the pyridone part is the included one, we found that the CN and Me groups of this moiety are too close to the atoms cage that repulsive interactions lead to a less stable complex. However, the energy difference between both nanostructures is small, and its value (1.6, 0.6, and 3.1 kcal /mol for the three above cavities, respectively) should be taken as indicative herein because of the approximation of the method and the absence of solvent contribution in the calculations. Scheme 2 shows a side view of the complexes having the minimum total energy following the first fitting mode.

SCHEME 2: Optimized Conformations of the 1:1 Complexes between MIR and CDs Using the PM3 Method[a]

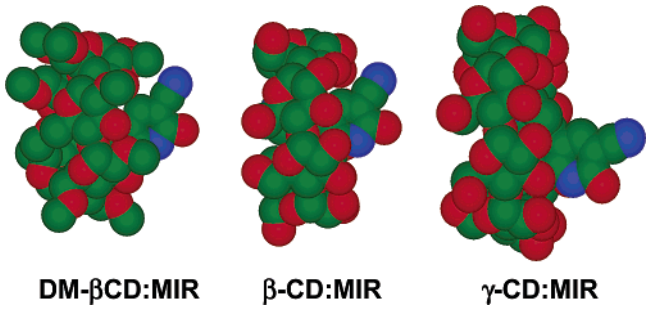

[a] For clarity, the hydrogen atoms of the complexes are not shown.

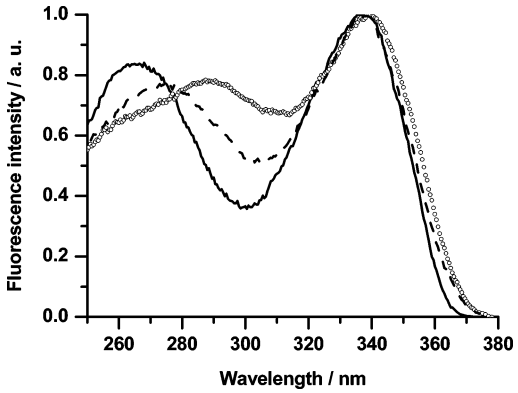

Figure 2. Excitation spectra of MIR in water (solid line) and in the presence of 16 mM of β-CD (- - -) and 21 mM of DM-β-CD (○○○). The emission wavelength is 390 nm.

The calculated value (using eq 1) of fluorescence quantum yield for DM-β-CD complex (∼0.08) is larger than that measured in pure water (0.014) and THF (∼0.005). We explain this result in terms of decrease in nonradiative processes of the encapsulated drug. In water, H-bonds, ICT, and twisting motion of the C−C bond connecting the two aromatic moieties affect the photophysics of MIR.[7] Previous X-ray crystallography and ^{1}H NMR studies showed that the **K** form is stable under a rotameric conformation in which the pyridyl part is rotated by 52.2° with respect to the main chromophore.[24] Confining MIR by CD reduces the efficiency of the above nonradiative channels. As said above, PM3 calculations suggest that the inclusion of MIR proceeds from the pyridyl moiety and part of the guest is located out of the cavity that twisting motion is possible (Scheme 2).

Figure 2 displays the fluorescence excitation spectra of the 385 nm emission band of MIR in neutral water and in the presence of β-CD and DM-β-CD. The shape of the spectra does not depend on the observed fluorescence wavelength. In neutral water, the excitation spectrum is similar to the absorption one. However, in the presence of DM-β-CD, the maximum of the $S_0 \rightarrow S_2$ band (∼270 nm) shifts by ∼23 nm (∼3000 cm^{-1}) to

longer wavelengths. The longest-wavelength absorption band ($S_0 \rightarrow S_1$ transition $\sim$ 340 nm) remains almost unaffected. The change around the 270 nm band indicates that the S_2 states of caged drug are subject to electronic changes due to a more stabilized structure upon encapsulation. The S_2 band of excitation spectrum shows a $\sim$1000 cm^{-1} red-shift in β-CD when compared to that recorded in DM-β-CD ($\sim$3000 cm^{-1}). For γ-CD complex, the shift is relatively smaller, $\sim$900 cm^{-1} (spectrum not shown). To explain these observations, we consider the solvent polarity effect on MIR absorption and emission spectra. We found (to be published) that, for example in 1,4-dioxane and acetonitrile, the S_2 band maximum appears at 275 and 315 nm, respectively. Most probably, the shift to longer wavelength in a polar solvent is reminiscent to the behavior of ^1L_b and ^1L_a inversion as in the case of several systems (indole, 1,2-methylindole, 1-aminonaphthalene, pyranine, and pyrenol).[25−28] Increasing the polarity of the medium makes ^1L_a more stable than ^1L_b. Encapsulation of MIR by CD precludes the formation of H-bonds between the N−H, C═O, and C≡N groups of the guest and water molecules. The lack of these interactions makes the ICT to CN group more efficient and therefore stabilizing the relevant state, in agreement with the larger shift in a more polar solvent (acetonitrile).

Another possibility to explain the shift of the $S_0 \rightarrow S_2$ transition to longer wavelength upon encapsulation or in polar solvents is the formation of a planar conformation in which a larger electronic delocalization at S_2 makes this state lower in energy. However, we notice that the $S_0 \rightarrow S_1$ band does not show any significant change which suggests that the electronic delocalization does not affect the S_1 energy much.

3.2. Picosecond Time-Resolved Emission Decays. Figure 3 displays representative emission spectra and decays of MIR in several media. Table 1 gives the results of the multiexponential fits to the fluorescence decays along with the data on absorption and emission spectra maxima. To begin with water solution, the decay could be fitted by a biexponential function giving time constants of $\sim$65 ps (99%) and $\sim$1.34 ns (1%).[7] Although the amplitude of the second component is rather small, the quality of the fit when this second component is added is significantly improved. The dominant short-decay component is due to the **K** structure and the minor nanosecond one represents the lifetime of the relaxed state of **K** due to an ICT reaction within the pyridone moiety.[7]

In Table 2, we give the fluorescence decay data at different β-CD concentrations. As expected, the values of the preexponential factors (a_2) of the inclusion complex emission component increases, while that of the free drug (a_1) decreases. In a parallel way, that of the relaxed ICT state contribution (a_3) slightly increases (from 1 to $\sim$5%). The hydrophobicity of the cavity interior plays a role in increasing the contribution of ICT character. Using DM-β-CD (Table 1), the decays of MIR become longer and three components were needed to get an accurate fit of the signal (Table 1). At 440 nm, the shortest (τ_1 = 76 ± 10 ps) and the longest (τ_3 = 1.22 ± 0.20 ns) decay times correspond to those already found in free aqueous solution (Table 1). An intermediate component (τ_2 = 350 ± 30 ps), whose relative contribution increases with CD concentration, is attributed to the lifetime of the caged drug. We notice that time-resolved measurements confirm the results obtained from steady-state spectral measurement indicating the existence of a 1:1 inclusion complex.

At 440 nm, the emission lifetime of the caged drug in β-CD ($\sim$235 ps (20%)) is comparable to that observed in γ-CD ($\sim$267 ps (22%)), but shorter than that observed for DM-β-CD ($\sim$350 ps (49%)). This result shows the effect of the methyl groups of the nanocapsule in the relaxation of the caged drug. Within β- and γ-CD, the drug is not deeply imbedded into the cage, and part of the guest (pyridone ring) is exposed to water molecules (Scheme 2). Furthermore, the guest may be subject to twisting motion of the pyridone moiety, and therefore a short emission lifetime is expected. Table 1 shows that the contribution of the nanosecond component increases from $\sim$1 to $\sim$9% upon inclusion of MIR in DM-β-CD nanocavity. This result suggests that the corresponding ICT state is sensitive to a further twisting motion of the pyridone part. Some restriction of the pyridyl ring rotation inside the nanocavity relatively increases the lifetime of the encapsulated structure. In a rigid PMMA solid film (Figure 3), the decay becomes longer and the fit gives three components with time constants of 5.4 ns (42%), 1.3 ns (27%), and 222 ps (31%). Due to the microscopic heterogeneity of the polymer due to the presence of different small domains with different sizes, it is normal to observe a rich emission decay. It is clear that the rigidity of the medium precludes twisting motion of the drug leading to longer emission lifetimes.

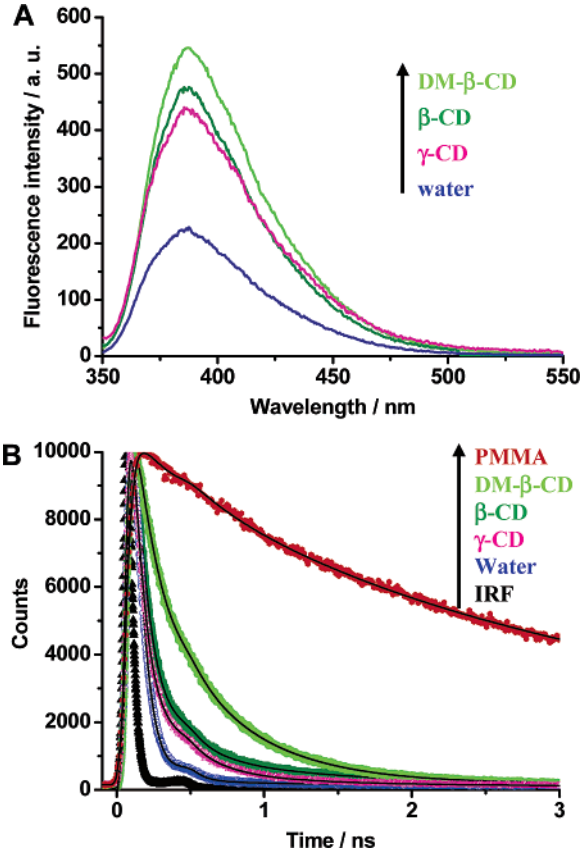

Figure 3. (A) Emission spectra of MIR in neutral water and in the presence of 16 mM of β-, γ-, and DM-β-CD, upon excitation at 340 nm. (B) Emission decays of the same solutions of part A gated at 440 nm and upon excitation at 371 nm. The data of the multiexponential fits are shown in Table 1.

In aprotic polar solvent (e.g. acetonitrile), the fluorescence quantum yield of MIR ($\sim$0.05) is larger than that observed in water ($\sim$0.014), suggesting the formation of hydrogen bonding between MIR and water plays a significant role in the photodynamics. In acetonitrile, the observed nanosecond component has a time constant of 1.1 ns, and the contribution of its amplitude increases to 12%. This result suggests that the relaxed ICT state is the origin of this component.[7] In acetonitrile, the lifetime of the picosecond component decreases to 30 ps (88%). In a non-hydrogen-bonding and less polar solvent, THF, the

TABLE 1: Values of the Emission Lifetimes (τ_i) and Normalized Pre-exponential Factors (a_i) from the Multiexponential Fit to the Fluorescence Decays of 1×10^{-5} M MIR at Different Wavelengths of Observation in Different Media[a]

solvent	[CD]/mM	λ_{obs}/nm	τ_1/ps	a_1	τ_2/ps	a_2	τ_3/ns	a_3	λ_A/nm	λ_F/nm
β-CD	16	390	66	0.87	245	0.12	1.52	0.01	266, 336	385
		410	71	0.78	234	0.19	1.55	0.03		
		440	61	0.75	235	0.20	1.56	0.05		
γ-CD	23	390	60	0.80	259	0.18	1.26	0.02	266, 336	385
		410	68	0.76	265	0.21	1.31	0.03		
		440	64	0.73	267	0.22	1.41	0.05		
DM-β-CD	21	390	76	0.50	353	0.44	1.22	0.06	266, 337	386
		410	76	0.43	348	0.48	1.20	0.09		
		440	76	0.42	350	0.49	1.22	0.06		
water		390	69	0.99			1.23	0.01	265, 336	385
		410	69	0.99			1.23	0.01		
		440	66	0.98			1.23	0.02		
THF		400	39	0.99			0.95	0.01	268, 350	397
		440	39	0.99			0.99	0.01		
PMMA		400	5410	0.42	222	0.31	1.34	0.27	270, 351	390
		440	5410	0.42	222	0.31	1.34	0.27		

[a] The table also contains the values of the wavelengths corresponding to the maximum of the UV−visible absorption (λ_A) and emission (λ_F) bands.

TABLE 2: Fitting Values for Emission Decays of MIR (2×10^{-5} M) at pH = 7 at Different Concentrations of β-CD

[β-CD]/mM	λ_{obs}/nm	τ_1/ps	a_1	τ_2/ps	a_2	τ_3/ns	a_3	χ^2
0	410	68	0.98			1.01	0.02	1.11
	440	68	0.98			1.12	0.02	1.17
5	410	72	0.87	235	0.09	1.29	0.04	0.99
	440	70	0.85	235	0.11	1.58	0.04	1.05
10	410	72	0.82	235	0.14	1.37	0.04	0.99
	440	71	0.80	235	0.16	1.55	0.05	1.20
16	410	71	0.78	235	0.18	1.46	0.04	0.99
	440	70	0.75	235	0.20	1.55	0.05	1.05

observed fluorescence lifetimes are 39 ps (99%) and ~1 ns (1%). These values are shorter than those observed in water (Table 1). Further nonradiative channels involving non-hydrogen-bonding interactions are also important for MIR relaxation in solution. These channels have their origin in the twisting of C−C bond between the two aromatic parts,[7] and are reduced in PMMA film. The emission of MIR in PMMA is intense, and its band does not show a significant shift when compared to those in water or CD solutions (not shown). Within the time resolution of the used apparatus (65 ps for IRF), we did not observe any ps rising component. Furthermore, under ps laser excitation (~0.3 mW and 20 MHz), the solutions were stable and did not show any new component due to possible photochemistry reactions between the drug and CD. This photobehavior might be useful when proposing CDs as solubilizers or nanocapsules for oral use formulation.

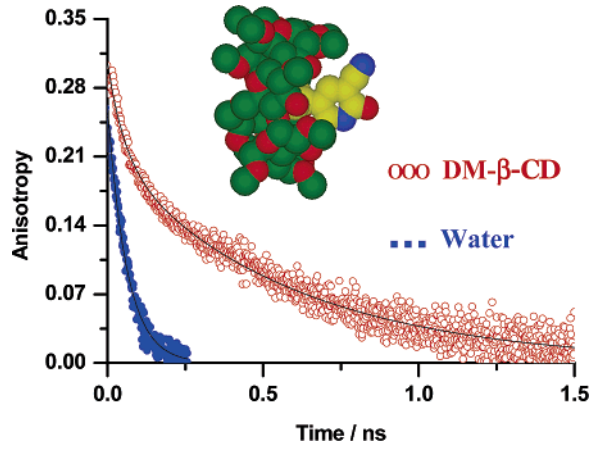

Figure 4. Anisotropy ($r(t)$) decay of MIR in water (●●●) and in an aqueous solution of 16 mM of DM-β-CD (○○○) upon excitation at 371 nm and observation at 460 nm. The results of the multiexponential fits (solid lines) are shown in Table 3. The inset shows the nanostructure of the 1:1 complex between MIR and DM-β-CD.

TABLE 3: Values of Rotational Time (ϕ_i) and Normalized Pre-exponential Factor (a_i) of Fluorescence Anisotropy Decay Fitting of MIR in Water, THF, and CDs[a]

solvent	ϕ_1/ps	a_1	ϕ_2/ps	a_2
water	67 ± 15	1		
THF	57 ± 15	1		
β-CD	48 ± 10	0.44	540 ± 50	0.56
γ-CD	43 ± 10	0.49	840 ± 70	0.51
DM-β-CD	60 ± 15	0.36	608 ± 50	0.64

[a] The excitation and observation wavelengths were 371 and 460 nm, respectively.

3.3. Anisotropy Decay and Structure of the Complexes. To get further information on the confined structure of MIR:CD, we have performed time-resolved emission anisotropy ($r(t)$) measurements in water, in CD solutions, and in THF. Figure 4 shows representative $r(t)$ decays for water and DM-β-CD solutions. Table 3 gives the results of $r(t)$-decays fitting. In pure water (and THF), the decay fits to a single-exponential function giving a rotational time ϕ= 67± 20 (and 57± 20 ps, respectively). Rotational times of 50 to 150 ps have been found for comparable (in size) aromatic molecules.[3,4,14,19,21,22,29−32] Within CD, the anisotropy decay of emission has a biexponential behavior, and it shows the existence of only 1:1 complex in agreement with the steady-state emission and lifetime data. For 15 mM DM-β-CD solution, the fit of $r(t)$ decay at 460 nm gives ϕ_1= 60 ± 20 (36%) and ϕ_2= 608 ± 50 ps (64%). These values are wavelength independent. ϕ_1 value is comparable to that found in THF (57 ps), and it may correspond to the rotational time of the drug. We attribute ϕ_2 to the rotational relaxation time of the 1:1 complex. However, because using 15 mM of DM-β-CD (K = 30 ± 5 M^{-1}) ~ 70% of the drug is not complexed, the short component should contain a significant

contribution from the rotational time in pure water (67 ps). For β-CD, we found $\phi_2 = 540 \pm 50$ ps. For γ-CD, we observed a relatively longer rotational time ($\phi_2 = 840 \pm 70$ ps), reflecting the difference in the complexes size. The initial value of $r(t)$ for the complexes $r(0) \sim 0.33$, is not far from the ideal one (0.4) and indicates that the emission transition moment of the caged drug has rotated by about 20° to that of its absorption.

Modeling MIR and the complex as a prolate ellipsoid and nonhydrated rotor, and using the hydrodynamics theory (eq 2),[33−37] we calculated the rotational time of these species.

$$\phi = \frac{\eta V(fC)}{k_B T} \tag{2}$$

In this expression, V is the molecular volume of the rotor (MIR or the whole complex), η is the viscosity of the solvent, k_B is the Boltzmann constant, T is the absolute temperature, and C is a constant depending on the boundary condition. The two limiting cases are the hydrodynamic stick and slip conditions. Under the stick one, the first layer of solvent "sticks" to the rotating body, therefore retarding its motion through the bulk viscosity. For slip boundary conditions, there is no tangential force exerted by the solvent on the rotating entity. The rotational motion is retarded only by the solvent which must be displaced as the body rotates. For a nonspherical solute molecule, the value of C follows $0 < C \leq 1$. It was observed that the magnitude of C depends on solute−solvent friction and on the relative size of the solute compared to the solvent molecules. The parameter f is a factor to account for the shape of the solute[36] ($f = 1$ for a sphere). For nonspherical molecules, $f > 1$ and the magnitude of the deviation from unity in the value of f describes the degree of the nonspherical nature of the solute rotor. Under stick limit conditions the value of f was determined from the molecular dimensions using the following expression:[34,37]

$$f = {}^2/_3 \frac{1 - \beta^4}{\frac{(2\beta^2 - \beta^4)}{\sqrt{1 - \beta^2}} \ln[{}^1/_\beta(1 + \sqrt{1 - \beta^2})] - \beta^2} \tag{3}$$

where $\beta = b/a$. a and b hold for semi-major and minor axis, respectively, of a prolate ellipsoid modeling CD complexes.

Therefore, the calculated orientation relaxation times of MIR in water under stick- and slip-boundary condition limits are 56 and 14 ps, respectively. The experimental value (67 ps in water) is close to the expected one under stick conditions, suggesting an attachment of the solvation shell to the drug. This result suggests the existence of strong H-bonding interactions between MIR and water molecules affecting its relaxation to the ground state.

To apply eq 2 to the complexes, the values of f and V ($4\pi abc/3$) were calculated from the molecular dimensions of the entities optimized by the PM3 method. For the MIR:β-CD complex, the results of the theoretical calculations give the axis values of the complex to be $a = c = 8.2$ Å, $b = 5.7$ Å, and $V = 1606$ Å^3. For the DM-β-CD complex, we obtained $a = c = 8.2$ Å (same as in β-CD), $b = 6.45$ Å, and $V = 1817$ Å^3. For the MIR:γ-CD complex, we obtained $a = c = 9.4$ Å, $b = 5.85$ Å, and $V = 2166$ Å^3.

Using the above dimensions of the nanostructures, we found $f = 1.09$, 1.16, and 1.26 Å for DM-β-, β-, and γ-CD complexes, respectively. The volume of MIR:CD complex is much larger than that of solvent (water) molecules. Therefore, we took the value of $C = 1$, which corresponds to a stick boundary condition. Taking into account the viscosity of the medium (water containing mM of CD) η (293 K) $\sim$ 1.1 cP,[38] and the value of the involved parameters, eq 2 gives the rotational time (ϕ_2) of the complexes under stick boundary conditionx and modeling these entities as a prolate ellipsoid. The obtained times are 508, 539, and 742 ps for β-, DM-β-, and γ-CD complexes, respectively. These values are within 90−95% close to the corresponding experimental ones (540 ± 50 ps for MIR:β-CD, 608 ± 50 ps for MIR:DM-β-CD, and 840 ± 70 ps for MIR:γ-CD, Table 3). Therefore, the theoretical and experimental data support each other, and the expected conformations of the complexes nanostructures from theory should not be very different from those in solution giving the observed spectra, emission lifetime, and rotational time constants.

4. Conclusion

The results of this study show the effect of CD confinement in the photophysical behavior of MIR. Within CD nanocages, the emission quantum yield increases and the lifetime of the drug becomes longer. The lifetime changes from ~65 ps in water to 240−350 ps using CD. The contribution of the minor nanosecond component due to the emission of a relaxed ICT state increases from 1 to ~9%. The changes are explained in terms of caging the pyridyl moiety of the drug leading to the formation of 1:1 inclusion complex in agreement with the results of PM3 calculations. The time-resolved anisotropy experiments gave more insight into the nature and structure of the complex. The conformation of the deduced structure is not different from that predicted by PM3 results. Following these results, the pyridone part of MIR is located outside the nanocapsule allowing further H-bonding interactions of the caged drug with water molecules as well as a twisting motion, leading to the short emission lifetime of the caged drug. Finally, under ps-laser excitation, we observed no photodegradation of the drug, a result which might be relevant to a possible use of CD:MIR complexes in pharmaceutical formulations.

Acknowledgment. This work was supported by the "Consejeria de Sanidad" of JCCM and MEC through projects SAN-04-000-00, CTQ2005-00114/BQU, and SAB2004-0086. M.E. thanks the MEC for the sabbatical year fellowship.

References and Notes

(1) Davis, M.; Brewster, M. *Nat. Rev. Drug Discovery* **2004**, *3*, 1023.
(2) Monti, S.; Sortino, S. *Chem. Soc. Rev.* **2002**, *31*, 287.
(3) Nandi, N.; Bhattacharyya, K.; Bagchi, B. *Chem. Rev.* **2000**, *100*, 2013.
(4) Douhal, A. *Chem. Rev.* **2004**, *104*, 1955.
(5) El-Kemary, M.; Douhal, A. Photochemistry and photophysics of cyclodextrin caged drugs. In *Cyclodextrin materials photochemistry, photophysics and photobiology*; Douhal, A., Ed.; Elsevier: 2006; Chapter 4.
(6) Bortolus, P.; Monti, S. *Adv. Photochem.* **1996**, *21*, 1.
(7) El-Kemary, M.; Organero, J. A.; Douhal, A. *J. Med. Chem.* **2006**, *49*, 3086.
(8) Altomare, C.; Cellamare, S.; Summo, L.; Fossa, P.; Mosti, L.; Carotti, A. *Bioorg. Med. Chem.* **2000**, *8*, 909.
(9) Krauze, A.; Vĩtolina, R.; Garaliene, V.; Sĩle, L.; Kluša, V.; Duburs, G. *Eur. J. Med. Chem.* **2005**, *40*, 1163.
(10) Bayliss, J.; Norell, M.; Canepa-Anson, R.; Reuban, S. R.; Poole-Wilsn, P. A.; Sutton, G. C. *Br. Heart J.* **1983**, *49*, 214.
(11) Siskind, S. J.; Sonnenblick, E. H.; Forman, R.; Scheuer, J.; LeJemtel, T. H. *Circulation* **1981**, *64*, 966.
(12) Benotti, J. R.; Grossman, W.; Braunwald, E.; Carabello, B. A. *Circulation* **1980**, *62*, 28.
(13) Weber, K. T.; Andrews, V.; Janicki, J. S.; Wilson, J. R.; Fishman, A. P. *Am. J. Cardiol.* **1981**, *48*, 164.
(14) Organero, J. A.; Tormo, L.; Douhal, A. *Chem. Phys. Lett.* **2002**, *363*, 409.
(15) Frisch, M. J. et al. *Gaussian 03*, revision B.05; Gaussian, Inc.: Pittsburgh, PA, 2003.

(16) Lee, C.; Yang, W.; Parr, R. G. *Phys. Rev. B* **1988**, *37*, 785−789.
(17) Connors, K. A. *Binding Constants: The Measurement of Molecular Stability*; John Wiley & Sons: New York, 1987; Chapter 12.
(18) Steiner, Th.; Saenger, W. *Carbohydr. Res*. **1995**, *275*, 73.
(19) Mondal, S. K.; Roy, D.; Sahu, K.; Sen, P.; Karmakar, R.; Bhattacharyya, K. *J. Photochem. Photobiol. A*: *Chem*. **2005**, *173*, 334.
(20) Gracía-Ochoa, I.; López. I. D.; Viñas, M. H.; Santos, L.; Ataz, E. M.; Sánchez, F.; Douhal, A. *Chem. Phys. Lett*. **1998**, *296*, 335.
(21) Sen, S.; Sukul, D.; Dutta, P.; Bhattacharyya, K. *J. Phys. Chem. A* **2001**, *105*, 10635.
(22) L. Tormo, L.; Organero, J.; Douhal, A. *J. Phys. Chem. B* **2005**, *109*, 17848.
(23) Rekharsky, M. V.; Inoue, Y. *Chem. Rev*. **1998**, *98*, 1875.
(24) Robertson, D. W.; Beedle, E. E.; Swartzendruber, J. K.; Jones, N. D.; Elzey, T. K.; Raymond, F.; Kauffman, H. W.; Wilson, H.; Hayes, J. S. *J. Med. Chem*. **1986**, *29*, 635.
(25) Dedonder-Lardeux, C.; Jouvet, C.; Perun, S.; Sobolewsk, A. L. *Phys. Chem. Chem. Phys*. **2003**, *5*, 5118.
(26) Szemik-Hojniak, A.; Balkowski, G.; Wurpel, G. W.; Herbich, J.; Van der Waals, J. H.; Buma, W. J. *J. Phys. Chem. A* **2004**, *108*, 10623.
(27) Trans-Thi, T.-H.; Prayer, C.; Millie, P.; Uznanski, P.; Hynes, J. T. *J. Phys. Chem. A*. **2002**, *106*, 2244.
(28) Suzuki, K.; Demeter, A.; Kühnle, W.; Tauer, E.; Zachariasse, K. A.; Tobita, S.; Shizuka, H. *Phys. Chem. Chem. Phys*. **2000**, *2*, 981.
(29) Zhong, D. P.; Douhal, A.; Zewail, A. H. *Proc. Natl. Acad. Sci. U.S.A.* **2000**, *97*, 14052.
(30) Hazra, P.; Chakrabarty, D.; Chakraborty, A.; Sarkar, N. *Biochem. Biophys. Res. Commun.* **2004**, *314*, 543.
(31) Dutt, G. B. *ChemPhysChem* **2005**, *6*, 413.
(32) Douhal, A. *Acc. Chem. Res*. **2004**, *37*, 349.
(33) Hu, C.; Zwanzig, R. *J. Chem. Phys.* **1974**, *60*, 4354.
(34) Baskin, J. S.; Zewail, A. H. *J. Phys. Chem. A* **2001**, *105*, 3680.
(35) Fleming, G. R. *Chemical Application of Ultrafast Spectroscopy*, Oxford University Press: London, 1986.
(36) Kalman, B.; Clark, N.; Johanson, L. B. A. *J. Phys. Chem*. **1989**, *93*, 4608.
(37) Perrin, F. *J. Phys. Radium* **1934**.
(38) Sen, P.; Roy, D.; Kumar, S.; Sahu, M. K.; Ghosh, S.; Bhattacharyya, K. J. *Phys. Chem. A* **2005**, *109*, 9716.